

Cluster synchronization in an ensemble of neurons interacting through chemical synapses

Masahiko Yoshioka*

*Brain Science Institute, The Institute of Physical and Chemical Research (RIKEN)
Hirosawa 2-1, Wako-shi, Saitama, 351-0198, Japan*

August 22, 2003
(Revised on May 18, 2005)

Abstract

In networks of periodically firing spiking neurons that are interconnected with chemical synapses, we analyze cluster state, where an ensemble of neurons are subdivided into a few clusters, in each of which neurons exhibit perfect synchronization. To clarify stability of cluster state, we decompose linear stability of the solution into two types of stabilities: stability of mean state and stabilities of clusters. Computing Floquet matrices for these stabilities, we clarify the total stability of cluster state for any types of neurons and any strength of interactions even if the size of networks is infinitely large. First, we apply this stability analysis to investigating synchronization in the large ensemble of integrate-and-fire (IF) neurons. In one-cluster state we find the change of stability of a cluster, which elucidates that in-phase synchronization of IF neurons occurs with only inhibitory synapses. Then, we investigate entrainment of two clusters of IF neurons with different excitability. IF neurons with fast decaying synapses show the low entrainment capability, which is explained by a pitchfork bifurcation appearing in two-cluster state with change of synapse decay time constant. Second, we analyze one-cluster state of Hodgkin-Huxley (HH) neurons and discuss the difference in synchronization properties between IF neurons and HH neurons.

1 Introduction

It has been revealed that periodically firing interneurons exhibit in-phase synchronization during the gamma oscillations (20-80 Hz) and the sharp wave burst (100-200 Hz) [1]. Interneurons are found to be connected through inhibitory chemical synapses. Therefore, a significant effort has been devoted to understand a role of inhibitory chemical synapses in in-phase synchronization in a large ensemble of neurons [2]. One major analytical approach to investigate synchronization of neurons is the phase reduction method, in which behavior of periodically firing neurons are reduced to the simple phase dynamics [3–6]. This phase reduction method is, however, applicable only to the case of weak couplings. To understand a role of strong couplings in synchronization of neurons we have to adopt different approach.

One difficulty in investigating strongly coupled neurons is time delayed interactions due to chemical synapses. Taking account of these time delayed interactions Hansel *et al.* have computed Floquet matrix and analyzed synchronization in a couple of strongly coupled neurons [4]. The size of this Floquet matrix, however, increases as the size of neural networks increases. Therefore, it is difficult to apply their approach to investigating the large size of neural networks.

Bressloff *et al.* have presented another scheme to deal with chemical synapses, which allows us to analyze stability of networks of integrate-and-fire (IF) neurons without computing the explicit form of Floquet matrix [5]. In some large size of neural networks they have found the degeneracy of eigenvalues, which makes it easy to analyze synchronization of many IF neurons. Actually, such degenerate eigenvalues in stability analysis are found not only in IF neurons but also in many synchronization phenomena induced by mean field interactions. A most prominent

*Electric Address: myosioka@brain.riken.go.jp

example of this degeneracy is seen in synchronization in an ensemble of chaotic oscillators such like Lorenz equations and logistic maps [7–10]. Just using the general properties of mean field interactions we can decompose linear stability of synchronous state of chaotic oscillators to two different components, which define the so called tangential Lyapunov exponents and transversal Lyapunov exponents. It must be noted that the result of this decomposition clearly indicates the occurrence of degeneracy regarding transversal Lyapunov exponents. Synchronization in many chaotic oscillators is thus characterized by only a small number of exponents included in tangential and transversal Lyapunov spectrum even if the system size is infinitely large.

In the present paper we employ these sophisticated reduction techniques in the chaos synchronization theory to investigate synchronization in the large number of neurons. The target of the analysis is cluster state, where an ensemble of neurons are subdivided into a few clusters, in each of which neurons exhibit perfect synchronization. To evaluate the degeneracy of eigenvalues we carry out the above-mentioned decomposition of a linear stability and define stability of mean state (tangential Floquet multipliers) and stabilities of clusters (transversal Floquet multipliers). Stability of mean state elucidates if cluster state is stable in the dynamics among clusters while stabilities of clusters clarify whether small perturbations in each cluster converge to vanish. We explicitly compute Floquet matrices of these stabilities for arbitrary neuron dynamics. Therefore, we can elucidate stability of cluster state for any types of neurons, even if the size of networks is infinitely large and neurons are connected through strong couplings.

To give a concrete example of the present stability analysis we first analyze networks of IF neurons interacting through uniform chemical synapses. In this analysis, we find the change of stability of a cluster, which elucidates that in-phase synchronization of a large ensemble of IF neurons occurs with only inhibitory chemical synapses. In addition, we investigate two clusters of neurons with different excitability, and discuss the relationship of their entrainment properties to the synapse decay time constant. Second, we analyze one-cluster state of Hodgkin-Huxley (HH) neurons and discuss the difference in synchronization condition between IF neurons and HH neurons.

The paper is organized as follows. In Sec. 2 we present the dynamics of neural networks that include Q clusters of spiking neurons. In Sec. 3, we present the analysis for cluster state of the neural networks. This analysis is applied to networks of IF neurons in Sec. 4. Then, we analyze synchronization of HH neurons in Sec. 5. Finally, in Sec. 6, we give a brief summary and discuss the future problems that can be solved by the present approach.

2 Networks of spiking neurons coupled with chemical synapses

We consider a spiking neuron whose state is represented by n -dimensional vector

$$\mathbf{x} = (v, w_1, w_2, \dots, w_{n-1})^T, \quad (1)$$

where v represent the membrane potential and $\{w_l\}_{l=1, \dots, n-1}$ describe gating of ion channels. Typically, the dynamics of a spiking neuron is defined by Hodgkin-Huxley (HH) equations, FitzHugh-Nagumo (FN) equations, and so on. We simply represent these neuron dynamics by

$$\dot{\mathbf{x}} = \mathbf{F}(\mathbf{x}). \quad (2)$$

In the analysis in Sec. 3, we assume spiking neurons in the form of Eq. (2). Nevertheless, in Sec. 4, we will investigate integrate-and-fire (IF) neurons, which cannot be expressed by Eq. (2) since v of IF neuron changes discontinuously. This discontinuity of IF neuron requires a minor corrections of the analysis in Sec. 3. We will discuss this minor correction in Sec. 4.

We assume that N spiking neurons $\{\mathbf{x}_i\}$ are interconnected through chemical synapses. To describe the dynamics of synaptic electric currents, we define spike timing by the time when membrane potential $v_i = [\mathbf{x}_i]_1$ (the first element of vector \mathbf{x}_i) exceeds the threshold value $\theta = 0$. We represent k -th spike timing of neurons i by $t_i(k)$, which satisfies

$$v_i[t_i(k)] = [\mathbf{x}_i[t_i(k)]]_1 = \theta \quad (3)$$

and

$$\dot{v}_i[t_i(k)] = [\dot{\mathbf{x}}_i[t_i(k)]]_1 > 0. \quad (4)$$

Then, the dynamics of networks of spiking neurons is expressed as

$$\dot{\mathbf{x}}_i = \mathbf{F}_i(\mathbf{x}_i) + (I_i, 0, \dots, 0)^\top, \quad (5)$$

where function $\mathbf{F}_i(\mathbf{x}_i)$ represents the dynamics of neuron i . Variable I_i represents a sum of synaptic electric currents, which is defined by

$$I_i = \sum_{j=1}^N J_{ij} \sum_{k=-\infty}^{\infty} S[t - t_j(k)], \quad (6)$$

where J_{ij} represents synaptic coupling from neuron j to neuron i , and function $S(t)$ describes time evolution of synaptic electric current. We assume $S(t)$ taking the form

$$S(t) = \begin{cases} 0 & t < 0, \\ \frac{1}{\tau_1 - \tau_2} (e^{-t/\tau_1} - e^{-t/\tau_2}) & 0 \leq t. \end{cases} \quad (7)$$

where $0 < \tau_2 < \tau_1$. Constants τ_1 and τ_2 are termed decay time and rise time, respectively.

2.1 Neural networks composed of Q clusters of neurons

In some problems, we have to consider neural networks including several clusters of neurons, such like networks including both interneurons and pyramidal neurons. Moreover, we will later study entrainment of two clusters of IF neurons that have different excitability between clusters. In the present study we analyze neural networks that are composed Q clusters of neurons. We assume that neurons share the same dynamical properties within each cluster, that is, we assume

$$\mathbf{F}_i(\mathbf{x}) = \mathbf{F}_q(\mathbf{x}), \quad i \in U_q, 1 \leq q \leq Q, \quad (8)$$

where U_q represents the set of neurons that belong to cluster q . In addition, we assume that synaptic couplings J_{ij} depend only on cluster indexes of pre and postsynaptic neurons, that is, we assume synaptic coupling J_{ij} of the form

$$J_{ij} = \tilde{J}_{qq'} / N, \quad i \in U_q, j \in U_{q'}. \quad (9)$$

Substituting Eqs. (8) and (9) into Eqs. (5) and (6) we obtain the dynamics of Q clusters of neurons:

$$\dot{\mathbf{x}}_i = \mathbf{F}_q(\mathbf{x}_i) + (I_q, 0, \dots, 0)^\top, \quad (10)$$

$$I_q = \frac{1}{N} \sum_{q'=1}^Q \sum_{j \in U_{q'}} \tilde{J}_{qq'} \sum_k S[t - t_j(k)], \quad i \in U_q. \quad (11)$$

Note that synaptic electric current in Eq. (11) depends only on cluster index q because of the assumption in Eq. (9).

3 Analysis

3.1 Cluster synchronization of periodically firing neurons

In the present analysis we focus on cluster state, in which spike timing of neurons are written in the form

$$\begin{aligned} t_i^*(k) &= t_q^*(k) = t_q^* + kT, \\ 0 \leq t_q^* &< T, \quad i \in U_q, \quad q = 1, \dots, Q, \end{aligned} \quad (12)$$

where asterisks indicates the quantity in stationary state. In this state, neurons emit periodic spikes synchronously within each cluster. We further assume that in cluster state not only spike

timing but also neuron states are synchronized within each cluster (i.e., $\mathbf{x}_i^* = \mathbf{x}_q^*$ ($i \in U_q$)). Substituting Eq. (12) into Eqs. (10) and (11), we obtain the dynamics of stationary state as

$$\dot{\mathbf{x}}_q^* = \mathbf{F}_q(\mathbf{x}_q^*) + (I_q^*, 0, \dots, 0)^\top, \quad (13)$$

$$I_q^* = \sum_{q'} \tilde{J}_{qq'} r_{q'} \tilde{S}(t - t_{q'}^*), \quad (14)$$

where $\tilde{S}(t)$ is defined by $\tilde{S}(t) = \sum_k S(t + kT)$ and $r_q = N_q/N$ represents the ratio of the number of neurons in cluster q to the total number of neurons.

To obtain the explicit form of cluster state we have to calculate T and $t_1^*, t_2^*, \dots, t_Q^*$ so as to obtain I_q^* and \mathbf{x}_q^* . It is obvious that we can safely assume $t_1^* = 0$, and we can calculate remaining Q unknown variables: $T, t_2^*, t_3^*, \dots, t_Q^*$ from Eqs. (13) and (14) following the same scheme as our previous study [11, 12]. Note that we can compute these variables not only for IF neurons but also for general neuron dynamics, as far as the stable cluster state is concerned.

3.2 Decomposition of linear stability

To investigate linear stability of cluster state we assume the infinitesimal deviations of state of neurons:

$$\mathbf{x}_i = \mathbf{x}_q^* + \delta \mathbf{x}_i, \quad i \in U_q \quad (15)$$

and infinitesimal deviations of spike timing:

$$t_i(k) = t_q^*(k) + \delta t_i(k), \quad i \in U_q. \quad (16)$$

From Eq. (3), we obtain

$$\delta t_i(k) = -\delta v_i[t_q^*(k)]/c_q = -[\delta \mathbf{x}_i[t_q^*(k)]]_1/c_q, \quad i \in U_q \quad (17)$$

with

$$c_q = v_q^*[t_q^*(k)] = [\dot{\mathbf{x}}_q^*[t_q^*(k)]]_1. \quad (18)$$

Note that constant c_q is independent of k because of the periodicity of the solution. To obtain the relation in Eq. (17), we must assume continuous neuron dynamics such as HH neurons and FN neurons. Note that we have to carry out the more careful calculation in discontinuous dynamics like IF neuron as we will discuss in Sec. 4. Expanding the dynamics in Eqs. (10) and (11) to the first order we obtain the dynamics for the deviations:

$$\delta \dot{\mathbf{x}}_i = \mathbf{F}'_q(\mathbf{x}_q^*) \delta \mathbf{x}_i + (\delta I_q, 0, \dots, 0)^\top, \quad (19)$$

$$\delta I_q = -\frac{1}{N} \sum_{q'} \sum_{j \in U_{q'}} \tilde{J}_{qq'} \sum_k S' [t - t_{q'}^*(k)] \delta t_j(k), \quad (20)$$

where $\mathbf{F}'_q(\mathbf{x}_q^*)$ denotes Jacobi matrix.

The naive evaluation of this $N \times n$ -dimensional dynamics yields an eigenvalue problem of the large size of matrix. Therefore, for each cluster, we define mean state of neurons:

$$\bar{\mathbf{x}}_q = \frac{1}{N_q} \sum_{i \in U_q} \mathbf{x}_i \quad (21)$$

and mean spike timing:

$$\bar{t}_q(k) = \frac{1}{N_q} \sum_{i \in U_q} t_i(k). \quad (22)$$

Noting Eqs. (19), (20), and (17), we can write the dynamics for $\delta \bar{\mathbf{x}}_q$ and $\delta \bar{t}_q(k)$ in the closed form

$$\delta \dot{\bar{\mathbf{x}}}_q = \mathbf{F}'_q(\mathbf{x}_q^*) \delta \bar{\mathbf{x}}_q + (\delta I_q, 0, \dots, 0)^\top, \quad (23)$$

$$\delta I_q = -\sum_{q'} \tilde{J}_{qq'} r_{q'} \sum_k S' [t - t_{q'}^*(k)] \delta \bar{t}_{q'}(k) \quad (24)$$

with

$$\delta\bar{r}_q(k) = -\delta\bar{v}_q[t_q^*(k)]/c_q = -[\delta\bar{\mathbf{x}}[t_q^*(k)]]_1/c_q. \quad (25)$$

Eqs. (23)-(25) define the decomposed stability of the original N -body stability. We term this decomposed stability stability of mean state. It must be noted that stability of mean state in Eqs. (23)-(25) is effectively a problem in a network of Q neurons with couplings $J_{qq'}r_{q'}$ since, to the first order, Eqs. (23)-(25) are equivalent to

$$\frac{d}{dt}(\mathbf{x}_q^* + \delta\bar{\mathbf{x}}_q) = \mathbf{F}_q(\mathbf{x}_q^* + \delta\bar{\mathbf{x}}_q) + (I_q, 0, \dots, 0)^\top, \quad (26)$$

$$I_q = \sum_{q'} \tilde{J}_{qq'} r_{q'} \sum_k S[t - t_q^*(k) - \delta\bar{r}_{q'}(k)]. \quad (27)$$

Stability of mean state is a necessary condition for the full stability, but not a sufficient condition. To investigate synchronization of neurons in each cluster we introduce deviations around the averaged state:

$$\mathbf{x}_i = \bar{\mathbf{x}}_q + \delta\tilde{\mathbf{x}}_i, \quad i \in U_q. \quad (28)$$

Subtracting Eq. (23) from Eq. (19) we obtain the dynamics of $\delta\tilde{\mathbf{x}}_i$ as

$$\delta\dot{\tilde{\mathbf{x}}}_i = \mathbf{F}'_q(\mathbf{x}_q^*)\delta\tilde{\mathbf{x}}_i, \quad i \in U_q. \quad (29)$$

Eq (29) defines another decomposed stability. We term this decomposed stability stability of a cluster. Stability of cluster q is satisfied when N_q deviations $\delta\tilde{\mathbf{x}}_i$ ($i \in U_q$) converge into $\mathbf{0}$. These N_q dynamics are, however, identical. Therefore, it suffices to evaluate one set of deviations to determine the stability of one cluster. Note that the determination of the stability of a cluster is effectively a problem of a single neuron dynamics under the unperturbed synaptic electric current I_q^* since, to the first order, Eq. (29) is equivalent to

$$\frac{d}{dt}(\mathbf{x}_q^* + \delta\tilde{\mathbf{x}}_i) = \mathbf{F}_q(\mathbf{x}_q^* + \delta\tilde{\mathbf{x}}_i) + (I_q^*, 0, \dots, 0)^\top, \quad i \in U_q. \quad (30)$$

3.3 Floquet matrices for stabilities of clusters

We can determine stabilities of clusters following the ordinary procedure of Floquet theory. Since the solution \mathbf{x}_q^* is periodic, $\mathbf{F}'_q(\mathbf{x}_q^*)$ is also periodic. Therefore, a solution of Eq. (29) is written in the form

$$\delta\tilde{\mathbf{x}}_i[t_q^*(k+1)] = \mathbf{M}_q^\perp \delta\tilde{\mathbf{x}}_i[t_q^*(k)], \quad i \in U_q. \quad (31)$$

Calculating Eq. (30) with small initial perturbations we can obtain every elements in matrix \mathbf{M}_q^\perp . $n \times n$ matrix \mathbf{M}_q^\perp has n eigenvalues $\{\lambda_{q\perp}^l\}_{l=1, \dots, n}$. When cluster q is stable, $\delta\tilde{\mathbf{x}}_i$ ($i \in U_q$) must converge to zero after a long time. Therefore, the stability of cluster q is fulfilled when the largest absolute eigenvalue $|\lambda_{q\perp}^1|$ satisfies the condition

$$|\lambda_{q\perp}^1| < 1. \quad (32)$$

3.4 Floquet matrix for stability of mean state

Determination of the stability of mean state is not an easy problem since the calculation of δI_q in Eq. (24) requires long past deviations of spike timing. To solve this problem, following Hansel *et al.* [4], we introduce the variables:

$$z_{q1} = \sum_{q'} \tilde{J}_{qq'} r_{q'} \sum_{t_q^*(k') < t} S[t - t_q^*(k') - \delta\bar{r}_{q'}(k')] \quad (33)$$

$$z_{q2} = \sum_{q'} \tilde{J}_{qq'} r_{q'} \sum_{t_q^*(k') < t} e^{-[t - t_q^*(k') - \delta\bar{r}_{q'}(k')]/\tau_1}. \quad (34)$$

By means of these variables we can exactly rewrite I_q in Eq. (27) in the truncated form

$$\begin{aligned}
 I_q &= \sum_{q'} \tilde{J}_{qq'} r_{q'} \sum_{t_q^*(k) \leq t_{q'}^*(k')} S \left[t - t_{q'}^*(k') - \delta \bar{t}_{q'}(k') \right] \\
 &\quad + e^{-[t - t_q^*(k)]/\tau_2} z_{q1} [t_q^*(k)] \\
 &\quad + S [t - t_q^*(k)] z_{q2} [t_q^*(k)], \quad t_q^*(k) < t.
 \end{aligned} \tag{35}$$

Therefore, δI_q is written as

$$\begin{aligned}
 \delta I_q &= - \sum_{q'} \tilde{J}_{qq'} r_{q'} \sum_{t_q^*(k) \leq t_{q'}^*(k')} S' \left[t - t_{q'}^*(k') \right] \delta \bar{t}_{q'}(k') \\
 &\quad + e^{-[t - t_q^*(k)]/\tau_2} \delta z_{q1} [t_q^*(k)] \\
 &\quad + S [t - t_q^*(k)] \delta z_{q2} [t_q^*(k)], \quad t_q^*(k) < t.
 \end{aligned} \tag{36}$$

This means that once we know $\delta z_{q1} [t_q^*(k)]$ and $\delta z_{q2} [t_q^*(k)]$, we can neglect past deviations of spike timing $\delta \bar{t}_{q'}(k')$ that arose before $t = t_q^*(k)$.

To take the advantage of z_{q1} and z_{q2} , we define the vector

$$\mathbf{y}_q = ([\bar{\mathbf{x}}_q]_1, \dots, [\bar{\mathbf{x}}_q]_n, z_{q1}, z_{q2})^\top. \tag{37}$$

We safely assume $t_q^* \leq t_{q+1}^*$ ($q = 1, \dots, Q-1$). Then, since Eq. (24) is equivalent to Eq. (36), from Eqs. (23), (36), and (25) we can show that deviation $\delta \mathbf{x}_q [t_q^*(k+1)]$ is determined from only $\delta \mathbf{y}_q [t_q^*(k)]$ and $\delta \bar{t}_{q'}(k_{qq'})$ with

$$k_{qq'} = \begin{cases} k & q \leq q', \\ k+1 & q' < q. \end{cases} \tag{38}$$

Moreover, deviations $\delta z_{q1} [t_q^*(k+1)]$ and $\delta z_{q2} [t_q^*(k+1)]$ are given as

$$\begin{aligned}
 &\delta z_{q1} [t_q^*(k+1)] \\
 &= - \sum_{q'} \tilde{J}_{qq'} r_{q'} S' \left[t_q^*(k+1) - t_{q'}^*(k_{qq'}) \right] \delta \bar{t}_{q'}(k_{qq'}) \\
 &\quad + e^{-T/\tau_2} \delta z_{q1} [t_q^*(k)] + S(T) \delta z_{q2} [t_q^*(k)],
 \end{aligned} \tag{39}$$

$$\begin{aligned}
 &\delta z_{q2} [t_q^*(k+1)] \\
 &= \frac{1}{\tau_1} \sum_{q'} \tilde{J}_{qq'} r_{q'} e^{-[t_q^*(k+1) - t_{q'}^*(k_{qq'})]/\tau_1} \delta \bar{t}_{q'}(k_{qq'}) \\
 &\quad + e^{-T/\tau_1} \delta z_{q2} [t_q^*(k)].
 \end{aligned} \tag{40}$$

Therefore, we can also determine $\delta z_{q1} [t_q^*(k+1)]$ and $\delta z_{q2} [t_q^*(k+1)]$ from the above mentioned variables: $\delta \mathbf{y}_q [t_q^*(k)]$ and $\delta \bar{t}_{q'}(k_{qq'})$. We can summarize these relationships in the form

$$\delta \mathbf{y}_q [t_q^*(k+1)] = \sum_{q'=1}^Q \mathbf{A}_{qq'} \delta \mathbf{y}_{q'} [t_{q'}^*(k_{qq'})] + \mathbf{B}_q \delta \mathbf{y}_q [t_q^*(k)], \tag{41}$$

where

$$\mathbf{A}_{qq'} = \left(\frac{\partial \delta \mathbf{y}_q [t_q^*(k+1)]}{\partial \delta \bar{t}_{q'}(k_{qq'})} \left(-\frac{1}{c_{q'}} \right) \quad \mathbf{0} \quad \dots \quad \mathbf{0} \right) \tag{42}$$

and

$$\mathbf{B}_q = \left(\frac{\partial \delta \mathbf{y}_q [t_q^*(k+1)]}{\partial [\delta \mathbf{y}_q [t_q^*(k)]]_1} \quad \dots \quad \frac{\partial \delta \mathbf{y}_q [t_q^*(k+1)]}{\partial [\delta \mathbf{y}_q [t_q^*(k)]]_{n+2}} \right). \tag{43}$$

In this equation, $\mathbf{A}_{qq'} \delta \mathbf{y}_{q'} [t_{q'}^*(k_{qq'})]$ represents the contribution from $\delta \bar{t}_{q'}(k_{qq'})$.

In Sec. 3.3, we obtain \mathbf{M}_q^\perp by calculating Eq. (30) with small perturbations. In the similar manner, we can compute \mathbf{A}_q and $\mathbf{B}_{qq'}$ explicitly for arbitrary neuron dynamics. We obtain $\partial \delta \mathbf{x}_q[t_q^*(k+1)]/\partial \delta \bar{t}_{q'}(k_{qq'})$ and $\partial \delta \mathbf{x}_q[t_q^*(k+1)]/\partial [\delta \mathbf{y}_q[t_q^*(k)]]_l$ by calculating Eqs. (26) and (35) with small perturbations. Partial derivatives of z_{q1} and z_{q2} have been given in Eqs. (39) and (40). Therefore, we can compute every elements in matrices \mathbf{A}_q and $\mathbf{B}_{qq'}$. For the further details of calculation of \mathbf{A}_q and $\mathbf{B}_{qq'}$ see Ref. [12](, though the definitions of \mathbf{A}_q , $\mathbf{B}_{qq'}$, and so on in Ref. [12] are slightly different from the present ones.)

We introduce vector

$$\mathbf{Y}(k) = (\mathbf{y}_1[t_1^*(k)]^\top \dots \mathbf{y}_Q[t_Q^*(k)]^\top)^\top. \quad (44)$$

Then, we can rewrite the relationship in Eq. (41) in the form

$$\delta \mathbf{Y}(k+1) = \mathbf{M}^\parallel \delta \mathbf{Y}(k) \quad (45)$$

with

$$\mathbf{M}^\parallel = \mathbf{M}_Q^\parallel \mathbf{M}_{Q-1}^\parallel \dots \mathbf{M}_1^\parallel, \quad (46)$$

where

$$\mathbf{M}_q^\parallel = \begin{pmatrix} \mathbf{E} & & & & & & & & \mathbf{0} \\ & \ddots & & & & & & & \\ & & \mathbf{0} & & & & & & \\ \mathbf{A}_{q1} & \dots & \mathbf{A}_{qq-1} & \mathbf{A}_{qq} + \mathbf{B}_q & \mathbf{A}_{qq+1} & \dots & \mathbf{A}_{qQ} & & \\ & & & \mathbf{E} & & & & & \\ & & \mathbf{0} & & & \ddots & & & \\ & & & & \mathbf{0} & & & & \mathbf{E} \end{pmatrix}. \quad (47)$$

Matrix \mathbf{M}_q^\parallel updates $\delta \mathbf{y}_q(k)$ to $\delta \mathbf{y}_q(k+1)$, and hence matrix \mathbf{M}^\parallel updates all the deviations. $Q(n+2) \times Q(n+2)$ matrix \mathbf{M}^\parallel has $Q(n+2)$ eigenvalues $\{\lambda_l^\parallel\}_{l=1, \dots, Q(n+2)}$, in which a trivial eigenvalue one is always included as in the case of ordinary Floquet matrix. The stability of mean state is satisfied when all other eigenvalues are less than one in absolute value, that is, the largest absolute eigenvalue $|\lambda_1^\parallel|$ and the second largest absolute eigenvalue $|\lambda_2^\parallel|$ satisfy

$$|\lambda_2^\parallel| < 1 = \lambda_1^\parallel. \quad (48)$$

4 Cluster synchronization in networks of integrate-and-fire (IF) neurons

Let us apply the above analysis to networks of IF neurons that are defined as

$$\dot{v}_i = -v_i + v_r + I_{\text{ext},q} + I_i, \quad i \in U_q. \quad (49)$$

When v_i exceeds the threshold value $\theta = 0$, v_i is reset to $v_0 = -1$. The resting potential v_r is set to $v_r = 1$, which leads intrinsic firing of neurons. We assume that these IF neurons are interconnected with uniform couplings:

$$J_{ij} = \frac{g}{N}. \quad (50)$$

As we have mentioned, the discontinuity of IF neurons require a minor correction of the stability analysis in Sec. 3. Since derivative \dot{v}_i changes discontinuously at spike timing, we define $c_q^- = \dot{v}_q^*[t_q^*(k) - 0]$ and $c_q^+ = \dot{v}_q^*[t_q^*(k) + 0]$. To take account of discontinuity of v_i , we extend the perturbed solution $v_q^* + \delta v_i$ before/after spike timing $t_i(k) = t_q^*(k) + \delta t_i(k)$ as illustrated in Fig. 1, and then define $\delta v_i^- [t_q^*(k)]$ and $\delta v_i^+ [t_q^*(k)]$. These deviations satisfy the condition,

$$\delta t_i(k) = -\delta v_i^- [t_q^*(k)]/c_q^- = -\delta v_i^+ [t_q^*(k)]/c_q^+. \quad (51)$$

We define two types of mean state variables: $\delta \bar{v}_q^- = (1/N) \sum_{i \in U_q} \delta v_i^-$ and $\delta \bar{v}_q^+ = (1/N) \sum_{i \in U_q} \delta v_i^+$, and two types of deviations around the mean state: $\delta v_i^- = \delta \bar{v}_i^- + \delta \tilde{v}_i^-$ and $\delta v_i^+ = \delta \bar{v}_i^+ + \delta \tilde{v}_i^+$.

Neuron i behaves continuously in the time interval $t_i(k) < t < t_i(k+1)$, during which we can carry out the decomposition of linear stability discussed in Sec. 3. Therefore, noting Eqs. (29), (49), and (51), we obtain

$$\delta\tilde{v}_i^-[t_q^*(k+1)] = e^{-T} \delta\tilde{v}_i^+[t_q^*(k)] = \frac{c_q^+}{c_q} e^{-T} \delta\tilde{v}_i^-[t_q^*(k)]. \quad (52)$$

Hence, matrix \mathbf{M}_q^\perp takes the form

$$\mathbf{M}_q^\perp = \left(\frac{c_q^+}{c_q} e^{-T} \right). \quad (53)$$

From Eq. (32), we obtain the condition for stability of cluster q :

$$\left| \lambda_{q1}^\perp \right| = \left| \frac{c_q^+}{c_q} e^{-T} \right| < 1. \quad (54)$$

Following the similar scheme, we can derive matrices $\mathbf{A}_{qq'}$ and \mathbf{B}_q . Substituting $\mathbf{A}_{qq'}$ and \mathbf{B}_q into Eqs. (46) and (47) yields \mathbf{M}^\parallel , by which we can determine the stability of mean state.

4.1 One-cluster state of IF neurons ($Q = 1$)

We begin with investigating one-cluster state $Q = 1$. In this state, all neurons take part in shaping one-cluster in-phase synchronization. One-cluster solution of Eqs. (13) and (14) is found with only $g < 1$ since too strong synaptic couplings with $g \geq 1$ leads bursting of neurons. To elucidate the stability of the solution with $g < 1$, assuming $\tau_1 = 3.5$, $\tau_2 = 0.1 \tau_1$, and $I_{\text{ext},1} = 0$, we calculate $|\lambda_1^\parallel|$, $|\lambda_2^\parallel|$, and $|\lambda_{11}^\perp|$ as a function of parameter g as shown in Fig. 2(a). Since the second largest absolute eigenvalue of \mathbf{M}^\parallel (i.e., $|\lambda_2^\parallel|$) is always less than one, the stability of mean state is always satisfied. However, the largest absolute eigenvalue of \mathbf{M}_1^\perp (i.e., $|\lambda_{11}^\perp|$) becomes greater than one with excitatory coupling $g > 0$. Therefore, the stability of a cluster is satisfied with only inhibitory coupling $g < 0$. These results imply that while a self-coupled single neuron ($N = 1$) can exhibit stable periodic firing with both inhibitory and excitatory couplings, in-phase synchronization of multiple neurons ($N > 1$) can take place with only inhibitory couplings $g < 0$. Since the networks show the same synchronization properties in all the decay time $\tau_1 > 0$, $\tau_1 - g$ phase diagram takes the simple form as described in Fig. 2(b). It turns out that in-phase synchronization of a large number of IF neurons occurs with only inhibitory synapses in all the value $\tau_1 > 0$.

Figure 3 shows the result of the numerical simulations. While the networks with inhibitory couplings ($g = -0.5$) exhibits the perfect in-phase synchronization, the network with excitatory couplings ($g = 0.5$) settles into the asynchronous state, in which neurons fire periodically with uniformly distributed phase shifts. Our stability analysis explains these numerical results well.

4.2 Two-cluster state of IF neurons ($Q = 2$ and $I_{\text{ext},1} = I_{\text{ext},2} = 0$)

We then investigate two-cluster state $Q = 2$ for inhibitory coupling $g < 0$ assuming $r_1 = r_2 = 0.5$ and $I_{\text{ext},1} = I_{\text{ext},2} = 0$. It has been shown that a couple of IF neurons exhibit a pitchfork bifurcation with change of synapse decay time constant [4]. We now show that this pitchfork bifurcation occurs even in systems of two clusters of neurons. Figure 4 shows $\tau_1 - \varphi_2$ bifurcation diagram, where φ_2 denotes t_2/T . There are three types of solutions: in-phase ($\varphi_2 = 0, 1$), anti-phase ($\varphi_2 = 0.5$), and out-of-phase solutions. Evaluating eigenvalues of \mathbf{M}^\parallel , \mathbf{M}_1^\perp , and \mathbf{M}_2^\perp , we find that the solutions denoted by thick lines satisfy the stability of mean state and the stabilities of clusters.

4.3 Entrainment of two clusters of IF neurons with different excitability ($Q = 2$ and $I_{\text{ext},1} = 0 \neq I_{\text{ext},2}$)

We extend the above result to investigate the case when the excitability of neurons are different between two clusters. Fixing $I_{\text{ext},1} = 0$, we investigate the behavior of φ_2 with change of $I_{\text{ext},2}$

in Fig. 5. With $I_{\text{ext},2} = 0$, we find three stable and two unstable solutions, which are consistent with the preceding results in Fig. 4. The in-phase solution $\varphi_2 = 0, 1$ is extended by the change of $I_{\text{ext},2}$ within the interval $-0.019 \lesssim I_{\text{ext},2} \lesssim 0.020$. In this interval two clusters of neurons show synchronized firing with small phase difference, that is, entrainment occurs. To examine the robustness of this entrainment, we plot this range of $I_{\text{ext},2}$ as a function of τ_1 in Fig. 6. The remarkable feature of this phase diagram is the narrow range of $I_{\text{ext},2}$ with short decay time constant τ_1 , and it is interesting that the pitchfork bifurcation described in Fig. 4 explains this narrow range of $I_{\text{ext},2}$. In this bifurcation diagram, the out-of-phase solutions merge into the in-phase solutions at $\tau_1 = 0$. Therefore, the entrained solution in Fig. 5 vanishes in the limit $\tau_1 \rightarrow 0$, and this vanishment explains the zero range of $I_{\text{ext},2}$ at $\tau_1 = 0$ in Fig. 6.

On the other hand, the out-of-phase solution ($\varphi_2 = 0.5$) is considerably robust against the change of $I_{\text{ext},2}$, especially with short τ_1 ($-0.083 \lesssim I_{\text{ext},2} \lesssim 0.080$ with $\tau_1 = 1.5$.) Nevertheless, when we apply the external currents to halves of neurons of both clusters (i.e., $Q = 4, r_1 = r_2 = r_3 = r_4 = 0.25, I_{\text{ext},1} = I_{\text{ext},3} = 0, I_{\text{ext},2} = I_{\text{ext},4} \neq 0, \varphi_1 = 0, \varphi_2 \sim 0, \varphi_3 \sim 0.5, \varphi_4 \sim 0.5$), the range for successful entrainment is found to be narrow ($-0.016 \lesssim I_{\text{ext},2} = I_{\text{ext},4} \lesssim 0.017$ with $\tau_1 = 1.5$). It seems that cluster synchronization easily breaks when we apply heterogeneous external electric currents that cause splitting of clusters.

5 One-cluster state ($Q = 1$) in networks of Hodgkin-Huxley (HH) neurons

To explore the biological plausibility of synchronization in IF neurons we study more realistic neuron model that is defined by HH equations. A HH neuron, whose dynamics is described in appendix A, does not show intrinsic firing without external stimulus. Therefore, we apply constant external electric current $I_{\text{ext}} = 10$ ($\mu\text{A}/\text{cm}^2$) to all of HH neurons and analyze synchronization in intrinsically firing homogeneous HH neurons assuming the same synaptic couplings as Eq. (50). Figure 7 shows $\tau_1 - g$ phase diagram, where the condition for stable one-cluster state ($Q = 1$ and $2 \leq N$) is described. In the large area of inhibitory couplings ($g < 0$) we find stable in-phase synchronization. Beyond $\tau_1 = 7.0$ the behavior of $|\lambda_2^{\parallel}|$ and $|\lambda_{11}^{\perp}|$ is similar to those of IF neurons described in Fig. 2(a), and the change of stability occurs at $g = 0$ because of $|\lambda_{11}^{\perp}|$. Below $\tau_1 = 7.0$, however, synchronization with inhibitory couplings takes place only below a certain negative value of g , and excitatory couplings can induce synchronization in some conditions. $\tau_1 - g$ phase diagram of IF neurons (Fig. 2(b)) can explain synchronization in HH neurons with slowly decaying synapses, though the synchronization condition of HH neurons with fast decaying synapses is more complicated than IF neurons.

6 Discussion

We have studied cluster state of networks of spiking neurons. We have shown the analytical method that can deal with synchronization in the large size of neural networks with arbitrary neuron dynamics and arbitrary interactions. Employing this analysis we have investigated networks of IF neurons interconnected through uniform chemical synapses. In the analysis of one-cluster state, we have found the change of stability of a cluster, which has elucidated that in-phase synchronization of multiple IF neurons occurs only with inhibitory couplings (Fig. 2). It must be noted that this analytical result well explains the structure of interneurons in the real nervous system, where interneurons are interconnected through inhibitory chemical synapses. In addition, we have investigated the entrainment of two clusters of IF neurons with different excitability (Fig. 6). We have explained the narrow range of $I_{\text{ext},2}$ with short decay time constant τ_1 in Fig. 6 by the bifurcation diagram described in Fig. 4. Furthermore, we have investigated one-cluster state of HH neurons. HH neurons show stable in-phase synchronization in the large parameter region of inhibitory chemical synapses, though the synchronization condition of HH neurons with fast decaying synapses is more complicated than IF neurons (Fig. 7).

Although van Vreeswijk *et al.* have proposed another type of stability criterion based on function $G(\phi)$ [14, 15], this stability criterion is unsound in some conditions. One counterexample of their criterion is a couple of IF neurons with couplings $J_{11} = J_{22} = -J_{12} = -J_{21} =$

$g/2$. With $\tau_1 = 3.5$ and $\tau_2 = 0.1\tau_1$, in-phase synchronization of these neurons becomes unstable beyond the critical point $g = 1.11$ as shown in Fig. 8. While our analysis based on linear stability precisely yields this critical point, van Vreeswijk's criterion, namely, $G(\phi) = -g(e^{-T}/2) \int_0^1 e^{T\theta} (\tilde{S}[T(\theta + \phi)] - \tilde{S}[T(\theta - \phi)]) d\theta$ with $T = \log(v_0 - v_r/v_0)$, fails to give the critical point. Gerstner *et al.* have also investigated networks of IF neurons [16]. Their analysis, however, cannot treat the realistic form of synaptic electric current $S(t)$ that exerts the long-time influence after activation within the finite size of matrix.

The present decomposition of linear stability is simple enough to investigate the general neuron dynamics including FN neurons and HH neurons. Even when the behavior of neurons are chaotic [17], we are still able to evaluate the stability of cluster state using tangential Lyapunov exponents and transversal Lyapunov exponents [18], and such technique may give a deeper understanding of the complicated behavior of HH neurons around the arrow in Fig. 7. It is interesting to apply the present analysis to networks including pyramidal neurons as well as interneurons [19]. The surface of the neocortex is subdivided into numerous columnar organizations, each of which is composed of several layers of neurons [20]. The internal and external dynamics of such columnar organizations would also be the future target of the present analysis.

A The Hodgkin-Huxley (HH) equations

The HH equations are the four-dimensional ordinary differential equations, which describe the spike generation of the squid's giant axon [13]. The dynamics of a neuron state vector $\mathbf{x} = (v, w_1, w_2, w_3)^T$ for a HH neuron is expressed as

$$C_m \dot{v} = \bar{g}_{Na} w_2^3 w_1 (v_{Na} - v) + \bar{g}_K w_3^4 (v_K - v) + \bar{g}_L (v_L - v) + I_{\text{ext}}, \quad (55)$$

$$\dot{w}_1 = \alpha_1 (1 - w_1) - \beta_1 w_1, \quad (56)$$

$$\dot{w}_2 = \alpha_2 (1 - w_2) - \beta_2 w_2, \quad (57)$$

$$\dot{w}_3 = \alpha_3 (1 - w_3) - \beta_3 w_3 \quad (58)$$

with

$$\alpha_1 = 0.01(10 - v) / \left\{ \exp\left(\frac{10 - v}{10}\right) - 1 \right\}, \quad (59)$$

$$\beta_1 = 0.125 \exp(-v/80), \quad (60)$$

$$\alpha_2 = 0.1(25 - v) / \left\{ \exp\left(\frac{25 - v}{10}\right) - 1 \right\}, \quad (61)$$

$$\beta_2 = 4 \exp(-v/18), \quad (62)$$

$$\alpha_3 = 0.07 \exp(-v/20), \quad (63)$$

$$\beta_3 = 1 / \left\{ \exp\left(\frac{30 - v}{10}\right) - 1 \right\}, \quad (64)$$

where $v_{Na} = 50$ [mV], $v_K = -77$ [mV], $v_L = -54.4$ [mV], $\bar{g}_{Na} = 120$ [mS/cm²], $\bar{g}_K = 36$ [mS/cm²], $\bar{g}_L = 0.3$ [mS/cm²], and $C_m = 1$ [μ F/cm²]. In the present study we set $I_{\text{ext}} = 10$ (μ A/cm²) to induce intrinsic firing of a HH neuron.

References

- [1] G. Buzsáki, Z. Horváth, R. Urioste, J. Hetke, and K. Wise, *Science*, 256, 1025 (1992).
- [2] X.J. Wang and G. Buzáki, *J. Neurosci.*, 16, 6402 (1996).
- [3] G.B. Ermentrout and N. Kopell, *SIAM J. Math. Anal.*, 15, 215 (1984).
- [4] D. Hansel, G. Mato, and C. Meunier, *Neural Comp.*, 7, 307 (1995).
- [5] P.C. Bressloff and S. Coombes, *Neural Comp.*, 12, 91 (2000).

- [6] Y. Kuramoto, Chemical oscillations, waves, and turbulence (Springer-Verlag 1984).
- [7] H. Fujisaka and T. Yamada, Prog. Theor. Phys. 69, 32 (1983).
- [8] K. Kaneko, Physica D, 77, 456 (1994).
- [9] Y. Maistrenko and T Kapitaniak, Phys. Rev. E, 54, 3285 (1996).
- [10] A. Pikovsky, O. Popovych, and Yu. Maistrenko, Phys. Rev. Lett., 87, 044102 (2001).
- [11] M. Yoshioka, Phys. Rev. E, 65, 011903 (2002).
- [12] M. Yoshioka, Phys. Rev. E, 66, 061913 (2002).
- [13] A.L. Hodgkin and A.F. Huxley, J. Physiol., 117, 500 (1952).
- [14] C. van Vreeswijk, L.F. Abbott, and G.B. Ermentrout, J. Comp. Neurosci, 1, 313 (1994).
- [15] C. van Vreeswijk, Phys. Rev. E 54, 5522 (1996).
- [16] W. Gerstner, J.L. van Hemmen, and J.D. Cowan, Neural Comp., 8, 1653 (1996).
- [17] U. Feudel, A. Neiman, X. Pei, W. Wojtenek, H. Braun, M. Huber, and F. Moss, Chaos, 10, 231 (2000).
- [18] M. Yoshioka, Phys. Rev. E, in press.
- [19] N. Kopell, G.B. Ermentrout, M.A. Whittington, and R.D. Traub, Proc. Natl. Acad. Sci. USA, 97, 1867 (2000)
- [20] V.B. Mountcastle, J. Neurophysiol. 20, 408 (1957)

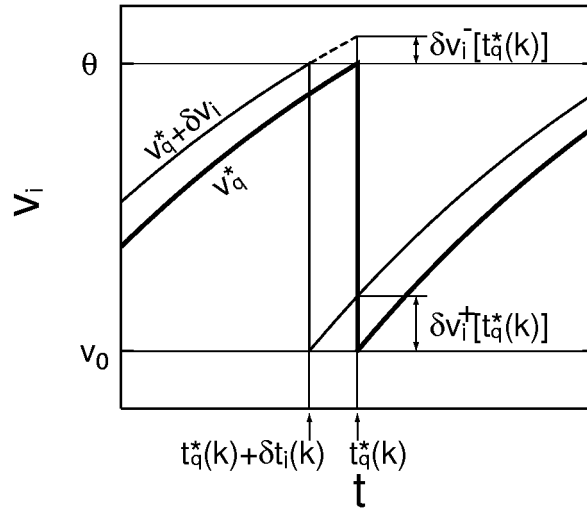


Figure 1: A schematic figure explaining the definition of $\delta v_i^- [t_q^*(k)]$ and $\delta v_i^+ [t_q^*(k)]$. Membrane potential of a IF neuron v_i changes discontinuously at spike timing $t_q^*(k) + \delta t_i(k)$. When $t_q^*(k) + \delta t_i(k) < t_q^*(k)$, we define $\delta v_i^- [t_q^*(k)]$ by extending the solution as shown in the figure, and we define $\delta v_i^+ [t_q^*(k)] = \delta v_i [t_q^*(k)]$. When $t_q^*(k) < t_q^*(k) + \delta t_i(k)$, we define these variables in the opposite way.

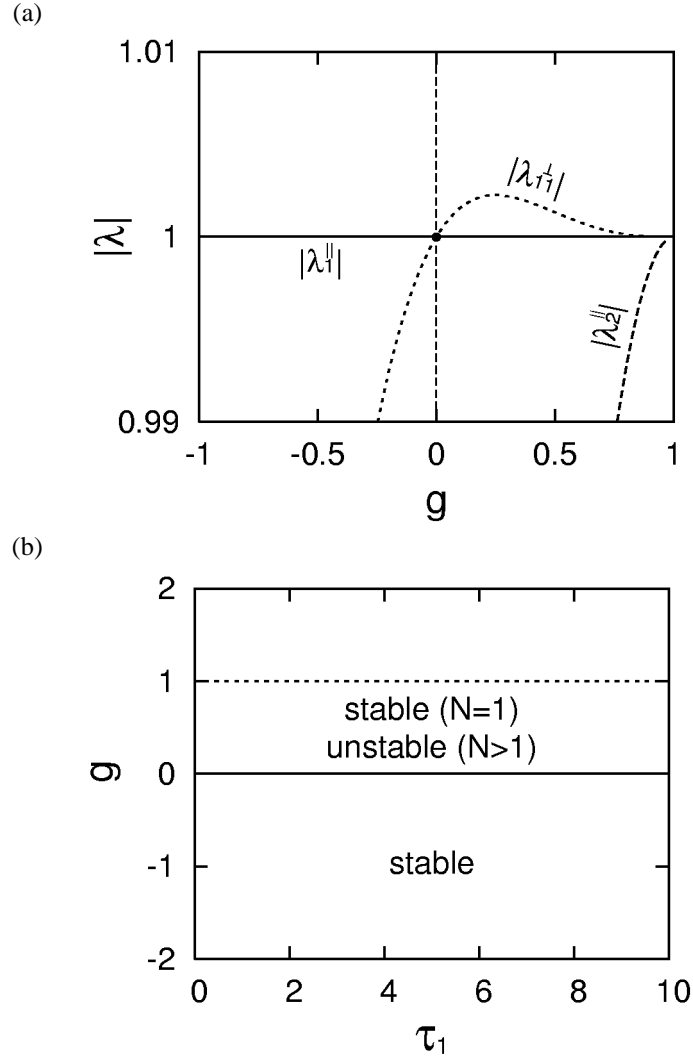


Figure 2: (a) Absolute values of λ_1^{\parallel} , λ_2^{\parallel} , and $\lambda_{1\perp}^{\perp}$ for one-cluster state ($Q = 1$) of networks of IF neurons are plotted as a function of g for $I_{\text{ext},1} = 0$, $\tau_1 = 3.5$, and $\tau_2 = 0.1\tau_1$. λ_1^{\parallel} always takes one while $|\lambda_2^{\parallel}|$ is always less than one. $|\lambda_{1\perp}^{\perp}|$ is less than one only when synapses are inhibitory ($g < 0$). These eigenvalues behave in the same manner even with the other decay time $\tau_1 > 0$. (b) τ_1 - g phase diagram, where we fix $\tau_2 = 0.1\tau_1$. A self-coupled single neuron ($N = 1$) has the stable periodic solution below $g = 1$. However, synchronization of multiple neurons ($N > 1$) occurs with only inhibitory couplings $g < 0$ since the stability of a cluster is fulfilled with only inhibitory couplings $g < 0$. Beyond $g = 1$, an excessive amount of positive synaptic electric current leads bursting of neurons.

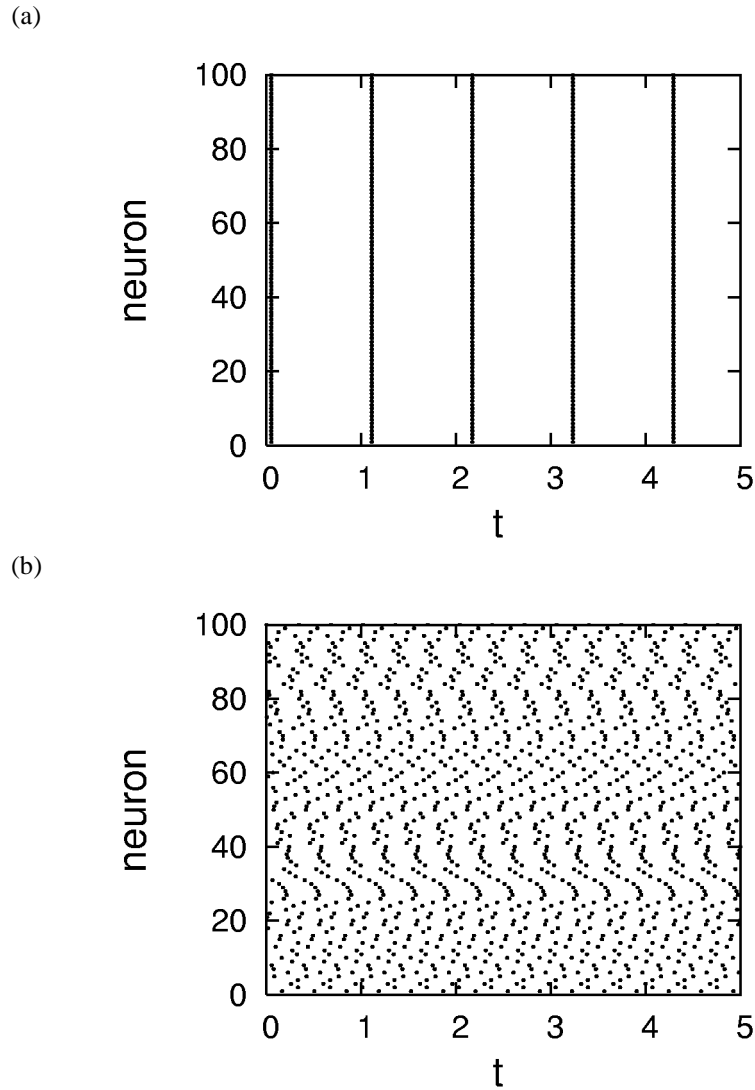


Figure 3: The result of numerical simulations with $N = 100$, $\tau_1 = 3.5$, and $\tau_2 = 0.1\tau_1$. Dots represent spike timing of neurons in a stationary state, which is realized after a long run of simulation. (a) With inhibitory synapses $g = -0.5$, the perfect in-phase synchronization occurs. (b) With excitatory synapses $g = 0.5$, we observe asynchronous state, in which neurons fire periodically with uniformly distributed phase shifts.

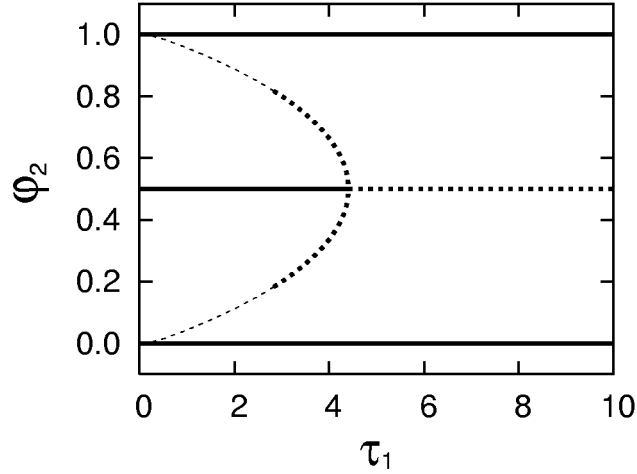


Figure 4: $\tau_1 - \phi_2$ bifurcation diagram for two-cluster state, where variable ϕ_2 denotes t_2/T ($Q = 2$, $1 \leq N_1 = N_2$, $g = -3$, $\tau_2 = 0.1\tau_1$, and $I_{\text{ext},1} = I_{\text{ext},2} = 0$.) The solutions represented by thick lines satisfy the stability of mean state and stabilities of clusters, while solutions represented by the dotted lines lack one or both of stabilities. The out-of-phase solutions plotted by the thin dotted line ($\tau_1 < 2.8$) is invalid since in these solutions membrane potential v_i crosses the threshold θ multiple times.

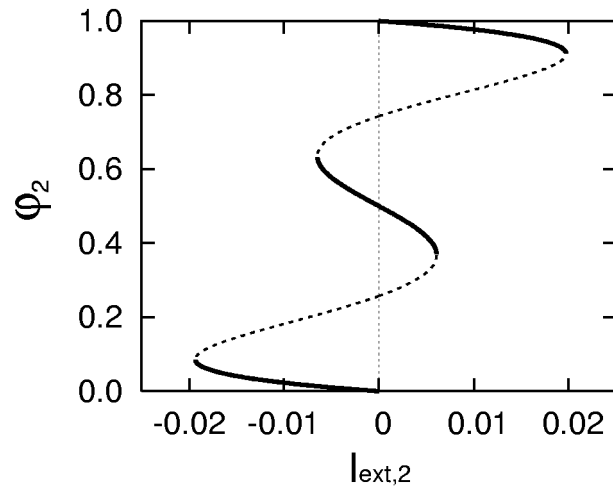


Figure 5: Entrainment of two clusters of neurons with different excitability. The solution ϕ_2 is plotted against $I_{\text{ext},2}$ for the fixed value of $I_{\text{ext},1} = 0$ ($Q = 2$, $1 \leq N_1 = N_2$, $g = -3$, $\tau_1 = 3.5$, and $\tau_2 = 0.1\tau_1$.)

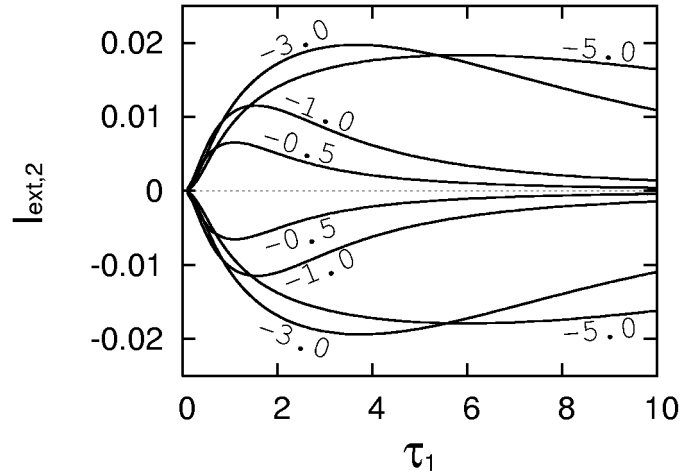


Figure 6: The upper and lower bounds of $I_{\text{ext},2}$ for entrainment of two clusters of neurons are plotted against τ_1 ($Q = 2, 1 \leq N_1 = N_2, \tau_2 = 0.1\tau_1$, and $I_{\text{ext},1} = 0$). The numbers in the figure indicate the value of g .

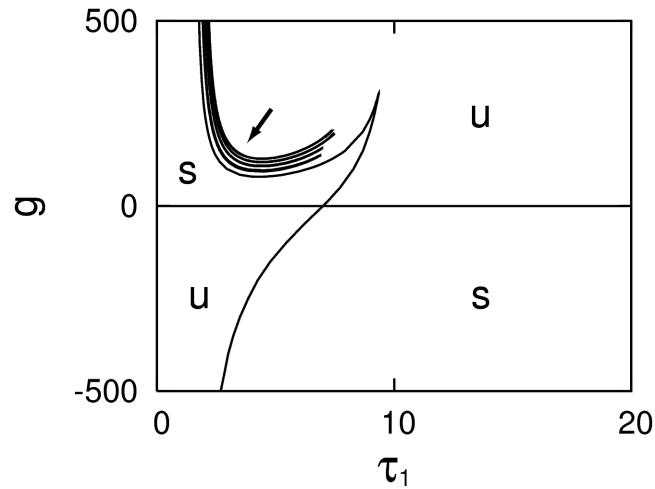


Figure 7: $\tau_1 - g$ phase diagram for one-cluster state ($Q = 1$) of multiple Hodgkin-Huxley (HH) neurons ($2 \leq N$) under the condition $\tau_2 = 0.1\tau_1$. “s” (“u”) in the figure indicates the region for the stable (unstable) one-cluster state. Around the arrow we find a lot of isolated regions for the stable one-cluster state. Note that we apply constant external electric current $I_{\text{ext}} = 10 (\mu\text{A}/\text{cm}^2)$ to all of HH neurons so as to induce intrinsic firing of neurons.

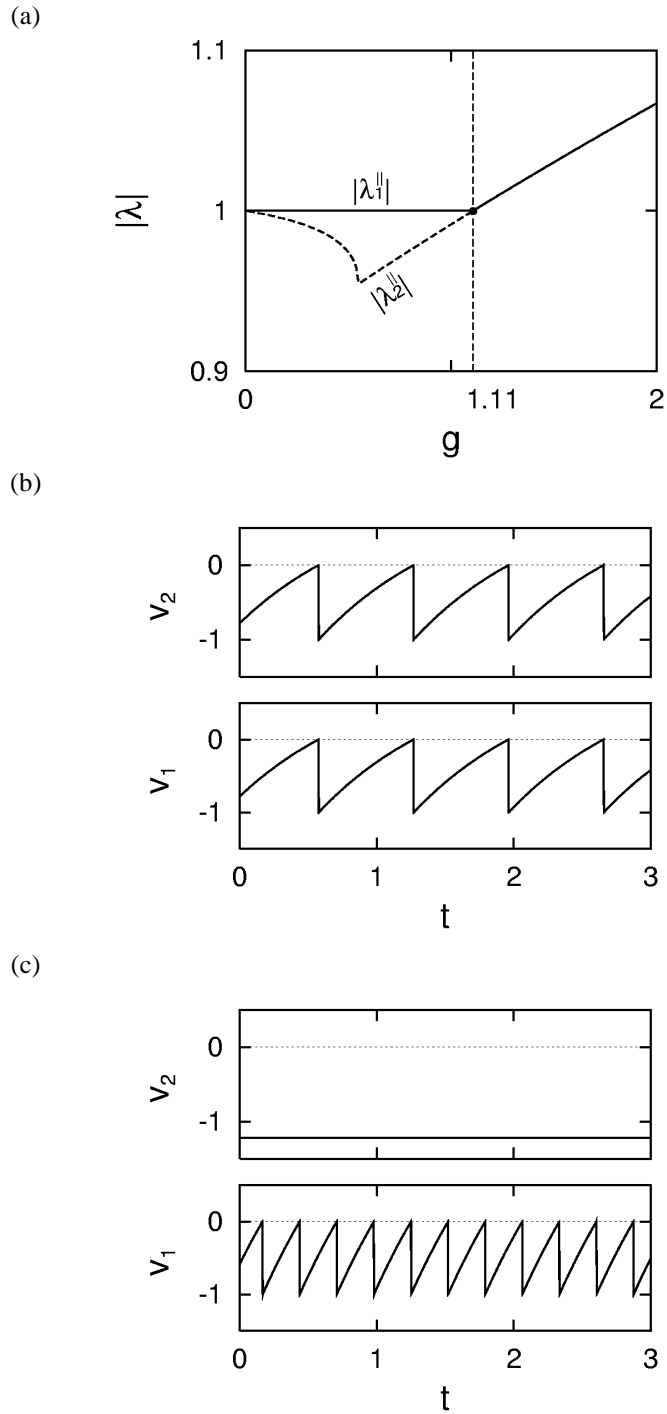


Figure 8: Stability of in-phase synchronization of a couple of IF neurons interconnected with $J_{11} = J_{22} = -J_{12} = -J_{21} = g/2$ ($\tau_1 = 3.5$ and $\tau_2 = 0.1\tau_1$). (a) Absolute values of λ_1^{\parallel} and λ_2^{\parallel} are plotted as a function of g . Beyond $g = 1.11$, the in-phase synchronization becomes unstable. (b) The result of numerical simulations with $g = 1.0$. A couple of neurons show in-phase synchronization. (c) The result of numerical simulations with $g = 1.2$. Only a single neuron fires at high frequency in the winner-take-all fashion.